Acta Universitatis Sapientiae
Electrical and Mechanical Engineering, 16 (2024) 149–161

DOI: 10.47745/auseme-2024-0013

Model Predictive Control of Aerodynamic Levitation Systems

Áron CZIMBALMOS[1], Áron FEHÉR[2], Lőrinc MÁRTON[2]

[1] Department of Mechanical Engineering, Faculty of Technical and Human Sciences,
Sapientia-Hungarian University of Transylvania, Tg. Mureş,
e-mail: aron.czimbalmos@gmail.com
[2] Department of Electrical Engineering, Faculty of Technical and Human Sciences,
Sapientia-Hungarian University of Transylvania, Tg. Mureş,
e-mail: {fehera, martonl}@ms.sapientia.ro

Manuscript received September 23, 2024; revised October 10, 2024

Abstract: Airjet-driven levitation systems are an important emerging technology, as they can ensure the contactless movement of objects. From a control engineering perspective, the position set-point tracking of the levitating object poses many challenges because the aerodynamic characteristics of the air jet used for levitation are difficult to model. The unmodelled disturbances significantly affect the control performances. Moreover, the bound constraints imposed by the mechanical design and the applied actuators should also be considered during controller design.

In this work, we present a motion control approach suitable for vertical levitation systems actuated by a fan-induced air jet. We developed the necessary hardware and software elements for the control equipment of the levitation system. We apply the MPC (Model Predictive Control) approach to ensure high-precision position regulation under various aerodynamic conditions with bounded control signals. We validate the applicability of the control system through simulation and real-time experimental measurements.

Keywords: Aerodynamic levitation, Model predictive control, constrained control, model-based control.

1. Introduction

Nowadays, we encounter control systems both in industrial implementations [13] and in household applications [10]. These systems can gather information from their environment and, by processing it, provide a real-time actuation for a controlled plant to achieve a prescribed objective [9].

A challenging control task is the implementation of the positioning in levitation systems. In these systems, a fan provides airflow that counterbalances the ball's weight. The ball hovers on the air cushion, which reduces friction and enables precise and stable movement of the ball within the tube, see *Fig. 1*.

Aerostatic bearings have several advantages over other bearing technologies [7]:

- They have low friction, which improves accuracy and efficiency;
- They do not require lubricants, which simplifies maintenance;
- They are lightweight.

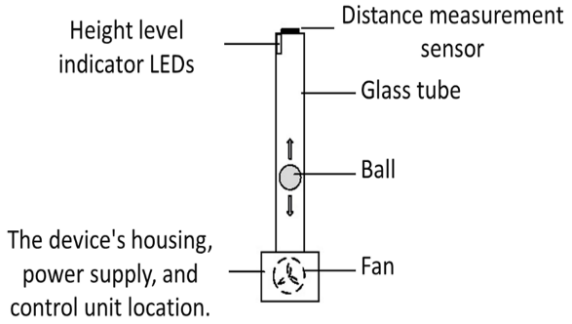

Figure 1: A schematic drawing of the levitation system

In the industry, for instance, air bearings can be used in 3D printing [14]. The technology can also be beneficial in material handling tasks, where levitating systems are used for the automated movement of objects [15]. These systems can also help to understand complex control methods effectively. Therefore, it can be used in education as a didactic tool since it is a relatively low-cost and spectacular demonstrative device [5]. Moreover, the ball levitation system can be applied for various entertainment purposes, such as demonstrations, concerts, or special events. Additionally, it can aid in perfecting "wind tunnels" or air chambers, which offer a great opportunity for individuals who want to experience the sensation of skydiving without any risk, expensive courses, or practical knowledge [4].

1.1. Previous Research

In earlier scientific papers discussing the implementation of such systems, classical PID control has been mostly used [12]. The PID controller design can be performed based on linearized input-output models, and they have the advantage of low computational costs. There are several similar implementations of such a levitation control approach. The paper [3] presents a low-cost air

levitation system to be used in both a virtual and a remote version. This work also proposes a linear single input single output model for controller design.

More complex levitation models were also developed. A dynamic skydiver levitation model and simulator is developed in [4], combining bio-mechanical, aerodynamic, and dynamic equations of motion.

To deal with non-linear physical behaviour exhibited by air-jet systems and to achieve high-precision and stable position control, advanced control methods such as those using artificial intelligence can also be applied [6].

1.2. Objectives

The aim of this work is to design and implement a levitation system that applies advanced control methods, which can be applied in education, industry, and even in the medical field for contactless, sterile movements with reduced frictional effects.

We hypothesize that by applying MPC (Model Predictive Control), we can implement a levitation system with outstanding set-point tracking and disturbance attenuation proprieties that can be utilized in education, industry, and even healthcare for contactless handling of levitation objects. The Model Predictive Control (MPC) system can achieve an optimal balance between implementation costs and high-precision tracking, even when disturbances are present.

2. System modelling

2.1 Equations of motion

Consider a ball under the influence of aerodynamic drag force, which ensures its levitation along a vertical tube. Its equation of motion along the vertical axis is given by:

$$m\ddot{x}(t) = F_{aero}(\mathrm{t}) - mg\ , \tag{1}$$

where x is the ball position, $m > 0$ is the mass of the ball, $g > 0$ is the gravitational acceleration, and t > 0 denotes the continuous time.

The aerodynamic drag force (F_{aero}) is produced by a rotating fan, and it depends on the difference between the ball velocity $\dot{x}$ and wind velocity v_w produced by the rotating fan. A quadratic force-velocity relation is assumed:

$$F_{aero}(\mathrm{t}) = b(v_w(\mathrm{t}) - \dot{x}(t))^2 \mathrm{sign}(v_w(\mathrm{t}) - \dot{x}(t))\ , \tag{2}$$

The parameter $b > 0$ depends on the ball's cross-section area, the aerodynamic drag coefficient, and air density.

Similar to previous studies, it is considered that the speed of the wind produced by the fan is proportional to the fan's angular velocity (ω), i.e.

$$v_w(\mathrm{t}) = K_w\omega(t) + C_w\,, \tag{3}$$

where $K_w, C_w > 0$ are constant parameters.

The angular speed of the fan is generated by an electromechanical actuator, with time constant $T_u > 0$ and static gain K_u. It is modelled as:

$$T_u\dot{\omega}(\mathrm{t}) + \omega(t) = K_u u(t)\,, \tag{4}$$

where u is the control input of the actuator (manipulated variable).

2.2 Control-oriented modelling

The controlled output of the process is the ball position (x), and the control input is the actuator motor input voltage u.

Based on the equations of motion, a state-space model can be formulated, which can be applied to controller design:

$$\begin{cases} \dot{\omega}(\mathrm{t}) = -\frac{1}{T_u}\omega(t) + \frac{K_u}{T_u}u(t) \\ \dot{x}(\mathrm{t}) = v(t) \\ \dot{v}(\mathrm{t}) = \frac{b}{m}\left(K_w\omega(t) + C_w - v(t)\right)^2 \mathrm{sign}\left(K_w\omega(t) + C_w - v(t)\right) - g \\ y(t) = x(t) \end{cases}. \tag{5}$$

Here y(t) denotes the controller output.

To obtain the dynamic relation between the input and the output, it is assumed that in equilibrium, the ball levitates around a (constant) equilibrium position x^*. In the case of the controlled system, this can be the prescribed controller set-point ($x_{ref}>0$).

The aerodynamic force (2) is linearized around this equilibrium:

$$F_{aero}(\mathrm{t}) \approx 2bv_w^*(K_w\omega(t) - \dot{x}(t))\,. \tag{6}$$

In the equilibrium state, the ball velocity is zero ($v^* = 0$). The corresponding fan speed is (ω^*) and equilibrium control input yields as:

$$\begin{cases} x^* = x_{ref} \\ v^* = 0 \\ \omega^* = \dfrac{1}{K_w}\left(\sqrt{\dfrac{mg}{b}} - C_w\right) \\ u^* = \dfrac{1}{K_u}\omega^* \end{cases}. \tag{7}$$

The linearized system model can be written as

$$\begin{cases}\dot{\mathbf{z}}(\mathrm{t}) = \mathrm{A}\mathbf{z}(\mathbf{t}) + \mathrm{B}u(t) \\ y(t) = Cz(t) + Du(t)\end{cases}, \tag{8}$$

where the state vector is

$$\mathbf{z} = (\omega(t) - \omega^* \quad x(t) - x^* \quad v(t) - v^*)^\top \text{ and,} \tag{9}$$

$$A = \begin{pmatrix} -\frac{1}{T_u} & 0 & 0 \\ 0 & 0 & 1 \\ 2\frac{bK_w}{m}(K_w\omega^* + C_w) & 0 & -2\frac{bv}{m}(K_w\omega^* + C_w) \end{pmatrix},$$

$$B = \left(\frac{K_u}{T_u} \quad 0 \quad 0\right)^\top,\ C = (0 \quad 1 \quad 0),\ D = 0\,. \tag{10}$$

It is easy to see that (A, B) and (A, C) are both full rank, so the linearised system is observable and controllable.

3. Controller design

2.1 Control objective:

*Le*t a constant prescribed position set-point $x_{ref} > 0$. Design the control input u such that $\lim_{t\to\infty}\left(x_{ref} - x(t)\right) = 0$. The ball's position and velocity are considered known (measurable).

To deal with the gravity-induced disturbance term and other unmodelled disturbances that could affect the motion dynamics, e.g. frictional disturbances in the actuator's mechanical transition or accidental tube wall–ball collision, a state feedback servo controller with integral term can be considered:

$$u(t) = K_P\left(x_{ref} - x(t)\right) - K_D\dot{x(t)} - K_\omega\omega(t) + K_I\int_0^t\left(x_{ref} - x(\tau)\right)d\tau\,, \tag{11}$$

where K_P, K_I, K_D, and K_ω are positive controller gains.

2.2 LQR (Linear Quadratic Regulator) design:

The control gains can be designed by considering the extended system, which includes the integral of the controlled position output:

$$\underbrace{\begin{pmatrix}\dot{\mathbf{z}}(t) \\ \dot{x}_I(t)\end{pmatrix}}_{\tilde{A}} = \underbrace{\begin{pmatrix}A & \mathbf{0} \\ C & 0\end{pmatrix}}_{\tilde{\mathbf{z}}}\underbrace{\begin{pmatrix}\mathbf{z}(\mathbf{t}) \\ x_I(t)\end{pmatrix}}_{\tilde{B}} + \begin{pmatrix}B \\ 0\end{pmatrix}u(t)\,, \tag{12}$$

where $\mathbf{0}$ is a zero-column vector with corresponding dimension, and x_I is the integral of the state x.

Based on this, the controller can be obtained by using an LQR approach: design the controller gains such that the control minimises the following functional:

$$J = \int_0^\infty (\tilde{\mathbf{z}}^T(\tau) Q \tilde{\mathbf{z}}(\tau) + R u^2(\tau))\, d\tau \,. \tag{13}$$

Here, $Q \in \mathbb{R}_{>0}^{4\times4}$ and $R \in \mathbb{R}_{>0}$ are design parameters.
The solution of the LQR problem is given by [8]:

$$\begin{cases} P\tilde{A} + \tilde{A}^T P + P\tilde{B}R^{-1}\tilde{B}^T P = -Q \\ K = R^{-1}\tilde{B}^T P \end{cases}, \tag{14}$$

where the controller gains are the entries of the row vector $K = (K_P\ K_D\ K_\omega\ K_I)$.

2.2 MPC (Modell Predictive Control) design:

It should also be considered that the control signal has to be always positive and is subject to an upper limit. Moreover, the controlled position state is also bounded. The boundedness of the control input and the controlled output can be considered by applying the MPC control approach [2]. MPC is a sophisticated control strategy extensively used in various industries to optimise the performance of complex processes. It involves predicting future process behaviour using a dynamic model and solving an optimisation problem at each control step to determine the optimal control actions. MPC can handle multi-variable systems and constraints effectively, making it invaluable for maintaining process variables within desired limits while maximising efficiency and productivity [11].

First, we discretised the model (8) using the forward-Euler scheme:

$$\begin{cases} z[k+1] = (T_s \mathrm{A} + I_3) z[k] + T_s \mathrm{B} u[k] \\ y[k] = Cz[k] + Du[k] \end{cases}, \tag{15}$$

where T_s is the sampling period, and *k = 0, 1, ...* denotes the discrete time.

Based on the discretised model (15), we designed a finite horizon model predictive controller that solves the following bounded optimisation problem:

$$\begin{aligned} \underset{u}{\text{minimise}} \quad & \textstyle\sum_{k=0}^{N} q\left(x_{ref} - y[k]\right)^2 + r_1 \Delta u[k]^2 + r_2 u[k]^2 \\ \text{subject to} \quad & M(u \quad \Delta u \quad y)^\top \le p \\ & z[k+1] = (T_s \mathrm{A} + I_3) z[k] + T_s \mathrm{B} u[k] \\ & y[k] = Cz[k] + Du[k] \end{aligned} \tag{16}$$

Although we created a finite horizon optimisation, the Meyer-term can be neglected since $x_{ref} - y[N] = 0$.

The terms in the inequality constraint are taken as:

$$M = \begin{pmatrix} 1 & 0 & 0 \\ -1 & 0 & 0 \\ 0 & 1 & 0 \\ 0 & -1 & 0 \\ 0 & 0 & 1 \\ 0 & 0 & -1 \end{pmatrix}, \; p = \begin{pmatrix} u_M \\ -u_m \\ \Delta u_M \\ -\Delta u_M \\ x_M \\ 0 \end{pmatrix}, \tag{17}$$

where u_M, u_m are the maximum and minimum values of the control signal, Δu_M is the maximum control rate, x_M is the maximum value of the position state. Since this implementation is an implicit MPC design, the controller solves the dynamic program (16) after every sampled data, then feeds the last value from the control sequence u into the plant.

If all of the states, outputs and inputs are bounded, an explicit MPC scheme can be formulated in the form

$$u[k] = Fz[k] + G\,, \tag{18}$$

where F, G matrices are state-dependent gain matrix and bias vector, respectively, with the appropriate dimensions [1].

4. Simulation measurements

To test the applicability of the Model Predictive Control approach on the levitation system, first, simulation experiments were performed in Matlab/Simulink environment. During the simulations, the dynamics of the process is considered to be described by the model (5). However, the linearised model (8) was applied for control design.

During the simulation the following system parameters were considered: $m = 27g,\; g = 9.81m/s^2,\; T_u = 1ms,\; K_u = 20,\; b = 9.202 \cdot 10^{-3},\; K_w = 1.979 \cdot 10^{-3}$, $C_w = 0.369$.

We used the set-point $x_{ref} = 25cm$ as the equilibrium point for linearisation.

In the optimisation problem (16), we chose the cost weights $q = 6.6502$, $r_1 = 0.0135$, first without the manipulated variable present in the cost function (i.e $r_2 = 0$), then with the manipulated variable also present (i.e. $r_2 = 0.02$). The manipulated variable was bounded in the interval $u \in [100{,}255]$, and the rate of the manipulated variable was bounded in the interval $\Delta u \in [-10{,}10]$. The output variable was kept in the physical boundaries $y \in [0{,}55]$.

The input and output bounds are cumulated in a vector as

$$p = (\,10\;\; -10\;\; 50\;\; 0\;\; 255\;\; -100)^T\,. \tag{19}$$

The prediction horizon was set to 8 samples, while the control horizon was kept at 2 samples. The MPC structure was created in MATLAB using the mpc function of the Model Predictive Control Toolbox, and the controlled system was simulated for 800 samples (equivalent to 8 seconds).

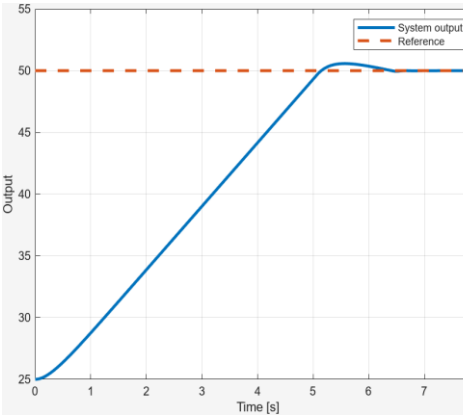

(a) Output trajectory of the controlled system

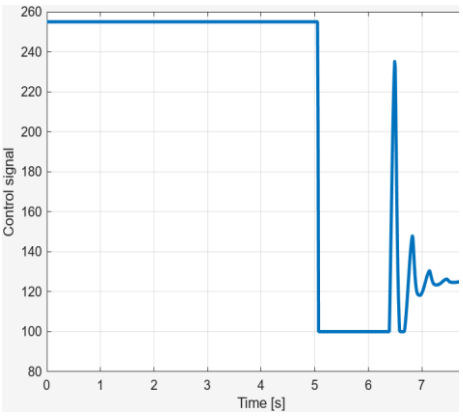

(b) Control signal output of the MPC

Figure 2: MPC control ($x_{ref} = 50$ cm, $r_2 = 0$)

Fig. 2a shows the reference signal and the controlled output of the closed loop system, while *Fig. 2b* shows the control signal when the control rate weight from (16) is $r_2 = 0$.

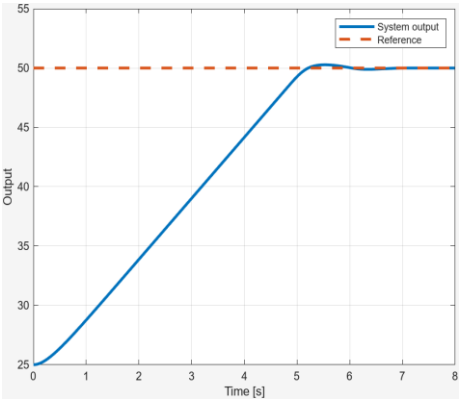

(a) Output of the controlled system

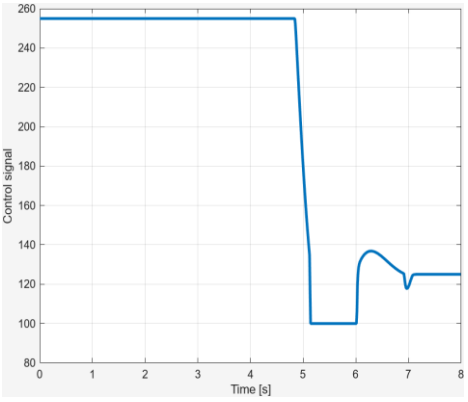

(b) Control signal output of the MPC

Figure 3: MPC control ($x_{ref} = 50$ cm, $r_2 = 0.02$)

Here, we can see that because of the unmodelled process, nonlinearities during controller design, overshot may appear during the transient state, but the control dampens it, ensuring precise steady-state reference tracking.

Fig. 3a shows the reference signal and the controlled output of the closed loop system, while *Fig. 3b* shows the control signal when the control rate weight is $r_2 = 0.02$. Adding a small penalty to the control signal dampens the controlled output. The output overshoot is smaller but the settling time is longer.

5. Experimental Measurements

5.1 Control Hardware

To implement the levitation control algorithm, an ESP32 microcontroller was applied, which reads data from distance sensors, an optical encoder, and a mechanical button. It displays output data on a screen and sends control signals to the motor via the motor controller. The electrical diagram of this equipment is shown in *Fig. 4.*

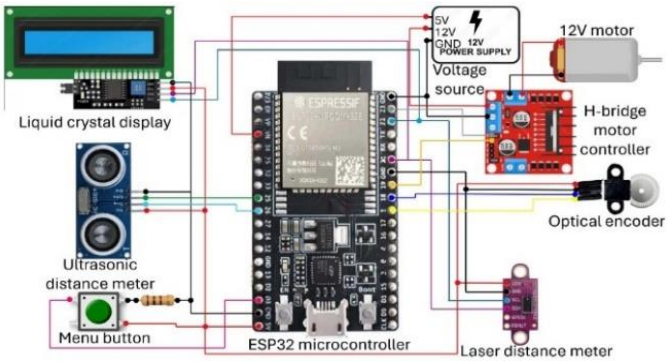

Figure 4: Electrical diagram of the control circuit

The *ESP32* is a highly popular microcontroller for control applications, known for its rapid processing capabilities and extensive built-in features. Thanks to its dual-core processor, it provides exceptional execution speed and can concurrently handle various tasks.

Due to its compact size, accuracy, and speed, we chose a *laser distance sensor* for distance measurement. The *VL53L0X* is a highly integrated laser distance sensor that uses Time-of-Flight (ToF) technology developed by STMicroelectronics for precise distance measurement. This sensor is small and has low power consumption, making it an ideal choice for applications where the space is limited and energy efficiency is important. For this reason, it was chosen to monitor the ball's position in the tube.

The system allows to set the reference height of the object by a moving human hand. Monitoring the hand position is done by an *HC-SR04* ultrasonic distance sensor. It provides an easy-to-use, reliable, and low-cost solution for distance measurement, which is why it is widely used in electronics, robotics, automation, and other fields.

The *fan* is powered by a *12V DC brushed motor*. The brushed DC motor is an excellent choice for low torque applications because it offers variable speed control capabilities. An *L298N* motor controller was necessary because the microcontroller's PWM (Pulse Width Modulation) duty cycle operates at a low voltage of 3.3V, while the motor's operating voltage is 12V. Using this module along with an external voltage source, we were able to easily control the motor from the microcontroller. To measure the motor's rotational speed, an incremental encoder was needed. For this purpose, we used a 100-resolution optical encoder. A 16x2 LCD and a push-button were utilised for displaying data and implementing a comprehensive menu system, allowing efficient human-machine interaction.

5.2 Mechanical setup

The levitation system is implemented in a metal-framed box with pressed plywood sides. Levitation occurs in a 55 cm long glass tube using a hairdryer fan.

We designed and 3D printed the necessary mechanical parts to secure the glass tube, the 2x16 LCD display, and the ultrasonic sensor. Two supporting components were needed for positioning and securing the fan and the encoder.

These parts were also custom-designed and then printed using a 3D printer. A 3D model of the entire assembly was created before implementation. This model is shown in *Fig. 5a*, and the built device is shown in *Fig 5b*.

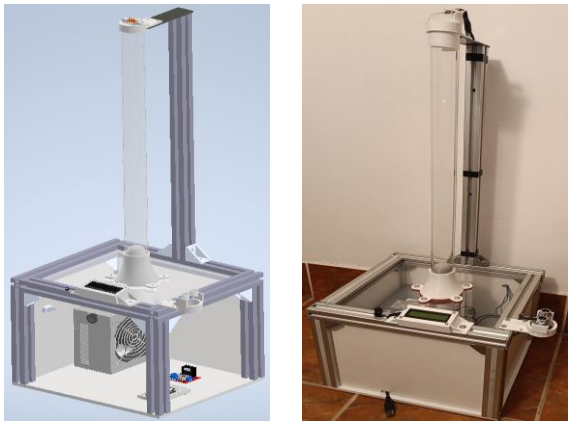

Figure 5: (a) 3D model of the equipment (b) Implemented equipment

5.3. Experimental results

Control experiments were performed on the presented levitation equipment to evaluate the applicability of the proposed control schemes.

The implementation form of the controller is given by the discretised form of the control algorithm (11), and it also takes into consideration the state and input constraints. In this case, the upper and lower bounds for the controlled state and controlled signal were chosen as $185 < u < 230$, $0 < x < 55$ (cm). The high value of the control signal's lower bound is motivated by the fact that under these values the wind speed generated by the fan is not able to initiate the motion of the ball.

It was taken into consideration that the time constant of the T_u is comparable to the applied sampling period, hence the dynamics in the first equation in (5) can be neglected, and $\omega \approx K_u u$. It yields that in the control (11) the term $K_\omega \omega$ can also be neglected. The controller parameters of the other terms are $K_P = 0.625$, $K_D = 13$, $K_I = 0.035$.

The experimental results are presented in *Fig. 6a* and *Fig. 6b* for $\boldsymbol{x_{ref} = 5\ cm}$. The simulation results show that despite the high-frequency measurement noises and unmodelled disturbances, e.g. accidental tube-ball collisions, the controlled system is capable of precise set-point tracking.

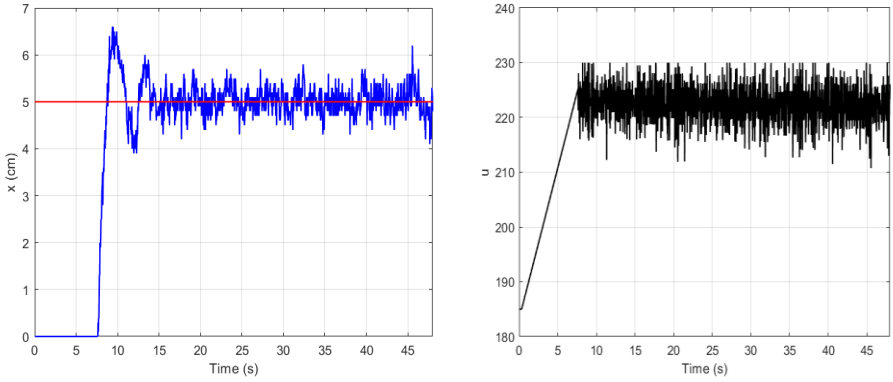

(a) Output trajectory (b) Control signal

Figure 6: Real-time measurements (x_{ref} *=5 cm*)

The control experiment was also performed for $x_{ref} = 50\ cm$. The same controller was applied as during the first control experiment. The experimental results presented in *Fig. 7a* and *Fig. 7b* show that similar steady-state tracking performances can be achieved as in the case of the previous experiments. During the transients, the effect of the applied control bounds can also be observed.

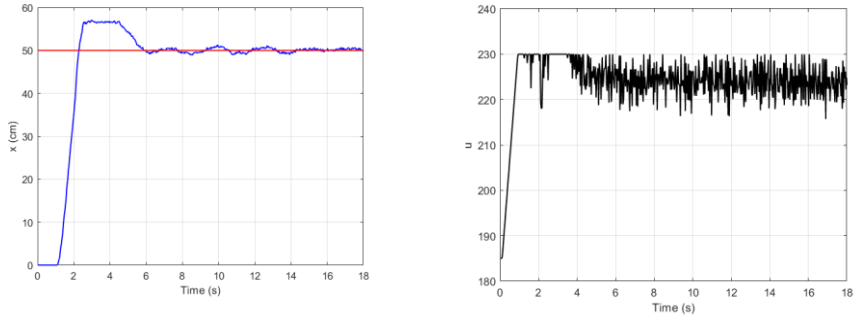

(a) Output trajectory (b) Control signal

Figure 7: Real-time measurements ($x_{ref} = 50$ cm)

6. Conclusions

Aerodynamic levitation is an effective technology for contactless actuation of delicate objects. In spite of the fact that the motion dynamics can be described by the classic Newtonian laws along one axis, the precise modelling of the aerodynamic force in the dynamic motion model can hardly be performed. This is why in the control-oriented modelling for motion control, disturbances should also be considered. On the other hand, it has to be taken into consideration, that the aerodynamic force is upper-bounded due to the fact that the electromagnetic actuator that rotates the fan can generate upper-bounded torques.

Acknowledgements

Publishing of this journal is supported by the Institute for Research Programmes of the Sapientia University. The first author's research was supported by Balassi Bálint Scholarship program.

References

[1] Bemporad, A., Pistikopoulos, E., Morari, M., and Dua, V., "The explicit solution of model predictive control via multiparametric quadratic programming", in *Proceedings of the 2000 American Control Conference. ACC (IEEE Cat. No.00CH36334)*, vol. 2, pp/ 872–876, 2000.

[2] Bemporad, A., Borrelli, F., and Morari, M., "Predictive Control for Linear and Hybrid Systems", *Cambridge University Press*, 2017.

[3] Esquembre, F., Chacon, J., Saenz, J., Diaz, J. M., and De la Torre, L., "Design of a low-cost air levitation system for teaching control engineering", *Sensors*, 17(10):2321, 2017.

[4] Clarke, A., and Gutman, P.-O., "A dynamic model of a skydiver with validation in wind tunnel and free fall", *IFAC Journal of Systems and Control*, 22:100207, 2022.

[5] de Oliveira Pedra, A. C., Caldeira, A. F., Maidana, C. F., Rech, C., and Venturini, S., F., "Feedback control applied to a low cost ball-in-tube air levitation plant", *Revista Ciencia e Natura*, 45, 2023.

[6] Garcıa, Y., "A self-tuning pid controller design based on fuzzy logic for nonlinear chemical processes", in *2020 IEEE ANDESCON*, pp. 1–6, IEEE, 2020.

[7] Singh, A. K., Arora, K., Jamwal, K. S., and Paswan, S. K., "Performance analysis of a designed aerostatic bearing with effect of surface roughness*", Iranian Journal of Science and Technology, Transactions of Mechanical Engineering*, pp. 1–19, 2023.

[8] Vrabie, D., Lewis, F. L., and Syrmos, V. L., "Optimal Control", *John Wiley & Sons*, 2012.

[9] Fehér, Á., and Márton, L., "Irányítástechnika. Laboratóriumi útmutató", *Scientia*, 2020.

[10] Ou, C.-H., and Rambe, K. H., "Enabling smart home energy management through gesture-based control and IOT technology", in *2023 International Conference on Consumer Electronics-Taiwan (ICCE-Taiwan)*, pp. 815–816. IEEE, 2023.

[11] Seborg, D. E., "Process Dynamics and control", *John Wiley Sons*, 2019.

[12] Jadlovska, A., Tkacik, M., Jadlovska, S., and Tkacik, T., "Design of aerodynamic ball levitation laboratory plant", *Processes*, 9(11):1950, 2021.

[13] Su, Q., Geng, Y., and Tu, Y., "Enabling secure and efficient data sharing and integrity auditing for cloud-assisted industrial control system", in *Big Data and Security: First International Conference, ICBDS 2019*, Nanjing, China, December 20–22, 2019, Revised Selected Papers 1, pages 514–528. Springer, 2020.

[14] Wiley, D., "Time Machined: Clocks, Values, and Digital Computation*", PhD Thesis*, New York University, 2021.

[15] El-Baz, D., Ning, H., and Zhu, L., "Survey on air levitation conveyors with possible scalability properties", in *2015 IEEE 12th Intl Conf on Ubiquitous Intelligence and Computing and 2015 IEEE 12th Intl Conf on Autonomic and Trusted Computing and 2015 IEEE 15th Intl Conf on Scalable Computing and Communications and Its Associated Workshops (UIC-ATC-ScalCom)*, pages 802–807. IEEE, 2015.